Clinical Usefulness of Fusion of ^{131}I SPECT and CT Images in Patients with Differentiated Thyroid Carcinoma

Yuka Yamamoto, MD; Yoshihiro Nishiyama, MD; Toshihide Monden; Yoshitaka Matsumura; Katashi Satoh, MD; and Motoomi Ohkawa, MD

Department of Radiology, Faculty of Medicine, Kagawa Medical University, Kagawa, Japan

Precise localization of the foci of ^{131}I uptake for management of patients with differentiated thyroid carcinoma can be difficult because of a lack of anatomic landmarks. The objective of the present study was to demonstrate the clinical usefulness of ^{131}I SPECT/CT fusion images in patients with differentiated thyroid carcinoma. **Methods:** CT and SPECT were performed 7 d after administration of a therapeutic dose of ^{131}I to 17 patients with differentiated thyroid carcinoma. External markers were placed at 3 locations on the skin of the patient to adjust the sections of CT and SPECT in the same geometric plane. Fusion images were constructed by combining the digital CT and SPECT images on a computer workstation. The data from both planar and SPECT ^{131}I images and CT images were first separately assessed by 2 nuclear medicine physicians. ^{131}I SPECT/CT fusion images were then interpreted. Fusion images were considered to improve image interpretation in comparison with CT and scintigraphy separately when they provided better localization of sites of increased radiopharmaceutical uptake. **Results:** Both CT and ^{131}I SPECT showed the pathologic sites in 5 of 17 patients (29%). Fusion images were considered to be of benefit in 15 of 17 patients (88%). In 4 patients, CT showed normal-sized lymph nodes, whereas ^{131}I SPECT showed abnormal findings. In 3 patients with bone metastasis, fusion images confirmed the precision of the localization of abnormal ^{131}I uptake. Five bone metastases and 1 muscle metastasis were occult and were not seen on the CT images. Finally, ^{131}I scintigraphy findings were abnormal for 2 patients for whom the CT findings were initially considered normal. Fusion images confirmed the precision of the localization of physiologic ^{131}I uptake. **Conclusion:** For registration of anatomic and functional images in fusion imaging, the method using external markers was simple and practical. ^{131}I SPECT/CT fusion images using this technique may improve anatomically limited interpretation of ^{131}I scintigraphy alone in patients with differentiated thyroid carcinoma.

Key Words: ^{131}I; CT; fusion image; thyroid carcinoma

J Nucl Med 2003; 44:1905–1910

Nuclear medicine imaging provides excellent information on functional biology. However, the anatomic information obtained from this technique is generally quite limited. In contrast, CT and MRI are excellent anatomic imaging modalities. Combination of the functional information from nuclear medicine imaging and the anatomic information from CT and MRI can improve diagnostic capability and facilitate image interpretation (*1*,*2*).

^{131}I scanning is indispensable for the management of patients with differentiated thyroid carcinoma (*3*). However, precise localization of the foci of ^{131}I uptake can be difficult because of a lack of anatomic landmarks. In addition, there are many other potential sites of physiologic uptake, such as the salivary glands, urinary bladder, gastrointestinal tract, and liver (*4*). Precise tumor localization for correct diagnosis and assessment of disease extent and metastatic spread is important for determining outcome in patients with thyroid carcinoma. SPECT should be performed to improve the sensitivity of ^{131}I imaging and to allow better localization of the tumor site. However, precise localization of tumor foci can still remain difficult despite optimal technical conditions and careful correlation with morphologic imaging. These difficulties may be related to various factors including lack of anatomic landmarks and physiologic distribution of the tracer.

Multimodality image coregistration can be achieved by several techniques using external markers or internal landmarks. Recently, CT combined with SPECT or PET has been developed (*5*–*7*). However, because of high cost, these systems are available in few centers and are limited to the combination of the above 3 modalities. The purpose of the present study was to demonstrate the clinical usefulness of ^{131}I SPECT/CT fusion images using external markers in patients with differentiated thyroid carcinoma.

MATERIALS AND METHODS

The study had 2 parts: a preclinical phantom study to validate the image fusion technique using CT and SPECT imaging systems, and a clinical feasibility study with 17 patients to assess the value of CT and ^{131}I SPECT image fusion.

Received Mar. 26, 2003; revision accepted Sep. 8, 2003.

For correspondence or reprints contact: Yuka Yamamoto, MD, Department of Radiology, Kagawa Medical University, 1750-1 Ikenobe, Miki-cho, Kita-gun, Kagawa 761-0793, Japan.

E-mail: yuka@kms.ac.jp

Preclinical Phantom Study

A cylindric phantom was prepared to check the accuracy and reproducibility of the methodology for registering CT and SPECT images. The phantom consisted of 5 ellipsis-shaped sources (5 cm long and 2 cm in maximum diameter) as internal landmarks filled with normal water and a ^{131}I solution with an activity of 25 kBq/mL for the CT and SPECT studies, respectively. The rest of the phantom was filled with normal water and a ^{131}I solution with an activity of 5 kBq/mL for the CT and SPECT studies, respectively. Three external markers (multimodality radiographic marker MM3003; IZI Medical Products) suitable for CT and SPECT scans were defined on the surface of the phantom. The MM3003 marker is disk shaped, with a sealant covering the top and forming a well in the center. For SPECT, ^{99m}Tc-pertechnetate (approximately 185 Bq per marker) was placed in the well of the external markers.

SPECT images were obtained using a dual-head γ-camera (Picker Prism 2000; Marconi Medical Systems) equipped with high-energy parallel-hole collimators. Acquisitions were performed with dual-energy windows: a 20% energy window centered at 364 keV for the ^{131}I images and a 20% window centered at 141 keV for the markers (^{99m}Tc). The data acquisition included a 360° rotation with 72 projections and a matrix of 64 × 64. CT images were obtained using multislice spiral CT scanning (Aquilion; Toshiba).

Clinical Feasibility Study

Patients. ^{131}I SPECT/CT fusion images after an oral therapeutic dose of ^{131}I (3.7–7.4 GBq) were obtained for 17 consecutive patients whose ^{131}I planar images showed an abnormality. The patients (8 male, 9 female; age range, 15–79 y; mean age, 49.5 y) had differentiated thyroid carcinoma (13 with papillary carcinoma, 4 with follicular carcinoma) and had undergone total thyroidectomy. Each patient gave informed consent for participation in the study.

CT. CT was performed 7 d after administration of a therapeutic dose of ^{131}I. Before CT acquisition, 3 external markers were placed at 3 locations: on the glabella and left and right axillary areas for neck SPECT; on the manubrium and left and right axillary areas for thoracic SPECT; around the umbilicus and the iliac crests for abdomen/pelvis SPECT; and on the pubic bone and left and right thighs for leg SPECT. While the patient was breathing naturally, multislice spiral CT (Aquilion) was performed on the lesion site that was suspected on the basis of ^{131}I planar images. The patients had their arms beside the body for neck imaging and behind the head for imaging of the thorax-to-leg region. The imaging protocol consisted of a 5- to 10-mm section thickness and a matrix size of 512 × 512.

^{131}I SPECT. ^{131}I SPECT was performed on the same day as CT. Images were obtained using a dual-head γ-camera (Picker Prism 2000; Marconi Medical Systems) equipped with high-energy parallel-hole collimators. Anterior and posterior spot imaging for 5 min and whole-body imaging at a speed of 9 cm/min were performed. SPECT was performed on the same day with the patient in a similar position, including arm position, as during the CT study and was focused on the suspected area of the lesion as seen on ^{131}I planar images. Before SPECT, ^{99m}Tc-pertechnetate (approximately 185 Bq per marker) was injected in each of the 3 markers on the skin. Acquisitions were performed with dual-energy windows: a 20% energy window centered at 364 keV for the ^{131}I images and a 20% window centered at 141 keV for the markers (^{99m}Tc). This yielded 2 simultaneously acquired sets of images: one showing the ^{131}I distribution and the other, the radioactive markers. The data acquisition included a 360° rotation with 72 projections and a matrix of 64 × 64. Iterative reconstruction was performed.

^{131}I SPECT/CT Fusion

Fusion images were constructed by combining morphologic CT and functional SPECT images on a computer workstation (Odyssey FX; Shimadzu). CT and SPECT data were transferred to the workstation by a DICOM network. The 2 sets of data were arranged to obtain a common matrix of 256 × 256. Datasets of CT and SPECT were fused using external landmarks and commercial software (Volume Registration; Shimadzu). The fusion algorithm of this program is based on the point-match method. With this method, up to 10 points in space can be marked manually as corresponding point pairs, within the CT volume data as well as within the SPECT volume data. If at least 3 point pairs are set, the coordinate system of the volume dataset of the SPECT image is translated and rotated in space in such a way that the sum of the squared distances of the point pairs is a minimum. After image fusion of the CT data and the resampled SPECT data, corresponding 5.6-mm-thick transaxial, coronal, and sagittal slices were obtained and simultaneously displayed, using a linked cursor. For fusion image display, an interlaced pixel approach was used, with CT images in gray scale and superimposed SPECT images in a bright color scale.

To quantitatively determine the accuracy of superimposition in the preclinical phantom study, the error of the point matching was shown as a root mean square (rms) of the point-pair distances in millimeters.

In the clinical study, data from both planar and SPECT ^{131}I images and CT images were first separately assessed by 2 nuclear medicine physicians. Tumor uptake of ^{131}I was defined as any focal or diffuse activity at sites incompatible with normal activity. A lymph node size of 10 mm in the short axis was used as a criterion for the presence of metastatic nodal involvement on CT. The ^{131}I SPECT/CT fusion images were then interpreted by the 2 physicians. Briefly, each individual CT abnormality was examined for pathologic ^{131}I uptake, and, conversely, suspected ^{131}I foci were compared with CT findings. Fusion images were considered to improve image interpretation in comparison with CT and scintigraphy separately when they better localized sites of increased radiopharmaceutical uptake. The gold standard for confirming the presence or absence of malignancy was surgery or clinical and radiologic follow-up of at least 6 mo.

RESULTS

Preclinical Phantom Study

Using the 3 external markers, the mean deviation expressed as rms in millimeters for CT/SPECT fusions was 2.65 ± 0.74 (±SD). This deviation was less than the intrinsic resolution of the SPECT image (7 mm).

Clinical Feasibility Study

All lesions in the present study could not be confirmed by surgery and were validated by radiologic and clinical follow-up of at least 6 mo.

CT and ^{131}I Scintigraphy Analysis Before Image Fusion. Both CT and ^{131}I scintigraphy showed the same pathologic sites in 5 of 17 patients (29%). However, it was difficult to

determine the precise location of the foci from SPECT images alone in 3 patients. In 2 patients, both imaging modalities showed abnormality in the mediastinal lymph node. In the remaining 12 patients, CT showed normal findings, whereas ^{131}I scintigraphy showed abnormal findings.

^{131}I SPECT/CT Fusion Data. Additional information for image interpretation was provided by ^{131}I SPECT/CT fusion images in comparison with CT and ^{131}I scintigraphy separately in 15 of 17 patients (88%). The details of imaging data are listed in Table 1. In 4 patients, CT showed normal-sized lymph nodes, smaller than 1 cm in diameter, whereas ^{131}I scintigraphy showed abnormal findings. In 3 patients with bone metastasis, fusion images confirmed the precision of the localization of abnormal ^{131}I uptake. Five bone metastases (Fig. 1) and 1 muscle metastasis (Fig. 2) were occult metastases and were not seen on the CT images. Finally, ^{131}I scintigraphy showed abnormal findings for 2 patients for whom the CT findings were initially considered normal. Fusion images confirmed the precision of the localization of physiologic ^{131}I uptake.

In 2 patients—patients 6 and 8 in Table 1—in whom bone metastasis with suspected nonosseous metastasis was detected separately on CT and SPECT, fusion images did not change the decision regarding the use of ^{131}I treatment but did influence the therapeutic dose of ^{131}I. In patients 14 and 15, on the other hand, fusion images excluded the tumor as the cause of uptake by showing the suspected focus to be in physiologic sites. These 2 patients were spared unnecessary treatment.

DISCUSSION

Using external markers, we have demonstrated the clinical usefulness of ^{131}I SPECT/CT fusion images in patients with differentiated thyroid carcinoma. Different imaging modalities provide different but complementary information. Both CT and MRI are used primarily for imaging anatomic changes associated with an underlying pathology, whereas the molecular imaging techniques of PET and SPECT capture functional or metabolic changes associated with the pathology. The use of anatomic and functional image fusion is increasing in nuclear medicine, and especially in oncology (*1*,*2*,*5*–*15*). Anatomic and functional information are combined to aid diagnosis, allow accurate tumor localization, and improve the outcome of treatment planning (*12*).

TABLE 1
Detailed Data for Patients for Whom Additional Information Was Provided by Fusion Imaging

Patient no.	Sex	Age (y)	Histologic type	^{131}I scintigraphy	CT/^{131}I SPECT	Additional information from CT/^{131}I SPECT
1	F	73	Papillary	Increased focal uptake in left neck	Uptake in left neck, normal-sized lymph node	Localization of lesion
2	M	76	Papillary	Increased focal uptake in upper mediastinum	Uptake in upper mediastinum, normal-sized lymph node	Localization of lesion
3	F	46	Papillary	Increased focal uptake in upper mediastinum	Uptake in upper mediastinum, normal-sized lymph node	Localization of lesion
4	F	24	Papillary	Increased focal uptake in upper mediastinum	Uptake in upper mediastinum, normal-sized lymph node	Localization of lesion
5	F	47	Papillary	Increased focal uptake in thoracic vertebra	Uptake in posterior portion of ninth rib	Detection of occult bone involvement
6	F	39	Papillary	Increased focal uptake in posterior midabdomen	Uptake in second lumbar spine	Detection of occult bone involvement
7	M	15	Papillary	Increased focal uptake in right pelvis	Uptake in right iliac wing	Detection of occult bone involvement
8	M	37	Papillary	Increased focal uptake in left upper mediastinum	Uptake in sternum	Detection of occult bone involvement
9	F	23	Papillary	Increased focal uptake in left thorax	Uptake in lateral portion of seventh rib	Detection of occult bone involvement
10	M	61	Follicular	Increased focal uptake in right pelvic bone	Uptake in right iliac wing	Localization of lesion
11	M	73	Follicular	Increased focal uptake in posterior midabdomen	Uptake in third lumbar spine	Localization of lesion
12	F	79	Follicular	Increased focal uptake in thoracic spine	Uptake in tenth thoracic spine	Localization of lesion
13	F	72	Papillary	Increased uptake in posterior part of right thigh	Uptake in biceps of right thigh	Detection of occult muscle involvement
14	F	39	Papillary	Increased uptake in lower abdomen	Uptake in urinary bladder (physiologic)	Localization of physiologic uptake
15	M	51	Papillary	Increased uptake in anterior lower neck	Uptake in site of tracheostomy (physiologic)	Localization of physiologic uptake

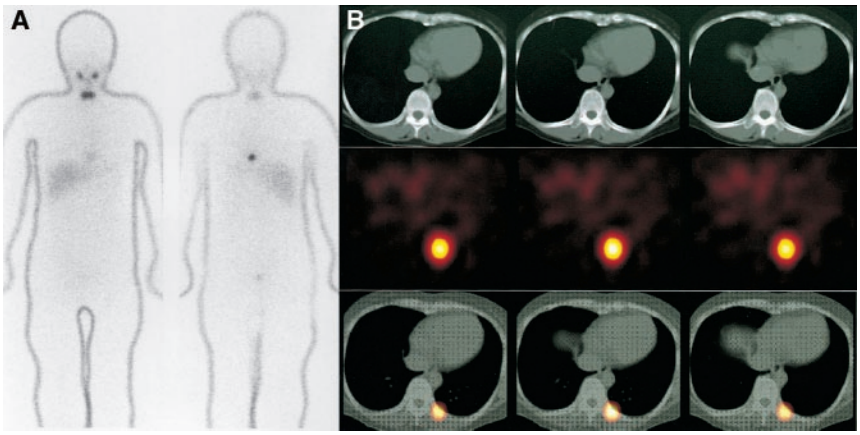

FIGURE 1. A 47-y-old woman (patient 5) with differentiated papillary thyroid carcinoma underwent total thyroidectomy. (A) ^{131}I whole-body images (left, anterior view; right, posterior view). (B) CT images (first row), ^{131}I transaxial SPECT images (second row), and ^{131}I SPECT/CT fusion images (third row). ^{131}I planar and SPECT images show intense focal uptake in posteromedial region, but slightly on left side of chest, suggesting thoracic spine involvement. Uptake in neck is thyroid bed. Bone appears normal on diagnostic CT scan. ^{131}I SPECT/CT fusion images show that intense tracer uptake is in posterior portion of 9th rib and not in thoracic vertebra. In this patient, final diagnosis was made on basis of follow-up; follow-up period was 12 mo, and clinically, fusion images confirmed precision of localization of abnormal ^{131}I uptake.

Whole-body imaging after an oral dose of ^{131}I is commonly performed to identify residual or metastatic tumor during the treatment of differentiated thyroid carcinoma. Scintigraphic procedures after administration of ^{131}I have a higher sensitivity for the detection of metastases from thyroid carcinoma than do anatomic imaging modalities. However, interpretation of ^{131}I images is difficult because of the absence of readily identifiable anatomic structures. Therefore, precise lesion localization is often not possible. In addition, knowledge about ^{131}I physiologic uptake is essential to avoid false-positive results in the interpretation of ^{131}I SPECT. It is also important for assessing additional ^{131}I treatment and monitoring the response to therapy. Correlation of anatomic and metabolic images is usually done visually by separate readings of CT/MRI and SPECT images. Misinterpretations can result, especially for small lesions. In the present study, ^{131}I SPECT/CT fusion imaging allowed precise localization of ^{131}I uptake in patients with differentiated thyroid carcinoma and, in comparison with separate analysis of CT and scintigraphy, improved the diagnosis in 15 of 17 patients (88%). In the abdominal and pelvic areas, ^{131}I SPECT/CT fusion imaging helped in differentiating physiologic urinary bladder elimination of ^{131}I from its abnormal uptake. The therapeutic dose of ^{131}I was changed in 2 patients because of the findings of fusion imaging. Two other patients were spared unnecessary treat-

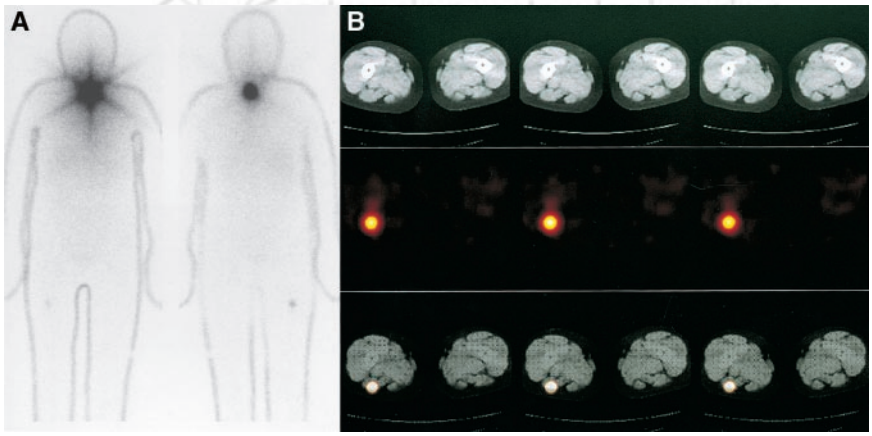

FIGURE 2. A 72-y-old woman (patient 13) with differentiated papillary thyroid carcinoma underwent total thyroidectomy. (A) ^{131}I whole-body images (left, anterior view; right, posterior view). (B) CT images (first row), ^{131}I transaxial SPECT images (second row), and ^{131}I SPECT/CT fusion images (third row). ^{131}I planar and SPECT images show focal uptake in posterior part of right thigh, suggestive of right femoral bone or muscle involvement. Intense uptake in neck is thyroid bed. Bone appears normal on diagnostic CT scan. ^{131}I SPECT/CT fusion images show that intense tracer uptake is located in biceps of right thigh and not in femoral bone. In this patient, final diagnosis was made on basis of follow-up; follow-up period was 9 mo, and clinically, fusion images confirmed precision of localization of abnormal ^{131}I uptake.

ment because of the fusion findings. For these 4 patients, the information provided by the image registration technique had an impact on management.

Perault et al. assessed the feasibility of registration with CT in 13 patients with endocrine carcinoma evaluated with ^{131}I, ^{131}I-MIBG, and ^{111}In-pentetreotide (*14*). The investigators obtained simultaneous dual-isotope acquisitions using these agents and ^{99m}Tc-methylene diphosphonate to get information on skeletal structures that could subsequently be correlated with anatomic data provided by CT. In their study, fused images allowed the detection and correct localization of 6 unsuspected sites of disease. At 2 sites, fusion led to better localization of known lesions; at 2 other sites, disease uptake was related to inflammatory changes seen on CT scans. The clinical value of combined transmission and emission tomography imaging was assessed using ^{131}I, ^{123}I-MIBG, ^{75}Se-cholesterol, ^{111}In-pentetreotide, and ^{99m}Tc-MIBI in 27 patients with endocrine tumors (*15*). For 41% of the patients, fused images improved the accuracy of nuclear medicine studies by providing better localization of SPECT-detected lesions. For one third of the patients, image fusion had a clinical impact on management.

Multimodality image coregistration can be achieved by several techniques using external markers or internal landmarks. Most fusion algorithms have been developed for brain imaging. The brain, being a rigid body, allows accurate registration (*16*). Internal landmarks relating to well-known sites of physiologic uptake have not been used with ^{131}I SPECT, probably because of the lack of reliable potential internal markers. In the present study, the method used external markers placed at specific positions on the patient's body. This method requires that CT and SPECT be performed on the same day, that the patient be imaged in the same position for both CT and SPECT, and that external markers be carefully matched. Respiration might affect that relationship, thus affecting the reliability and usefulness of the registration process. In our study, CT and SPECT were both performed while the patients were breathing freely. This was possible even in moderately cooperative patients, because of the short scanning time of helical CT. In point matching, the transformation parameters were determined by establishing a correspondence between a set of landmarks visible in both imaging modalities and minimizing the mismatch between these points. The rms error of 2.65 mm obtained in this study appears to be sufficient in view of the SPECT resolution. The accuracy obtained with the markers described here should be sufficient for image fusion of CT and SPECT. One partial solution to positioning problems is provided by integrated SPECT/CT or PET/CT systems that acquire both anatomic and functional information in the same examination (*5*–*7*). These systems allow the patient to be imaged in exactly the same position, reducing the artifacts that occur because of unavoidable minimal differences in positioning when CT and SPECT are performed successively. However, combination of the 2 modalities in the clinical setting is associated with many practical problems, such as high cost and lack of availability.

Realignment is fast when external markers are used, and a technologist trained to work with the realignment software can perform the entire procedure in less than 10 min. For clinically oriented settings, establishing such a method may be a cost-effective alternative to investment in a combined SPECT/CT device. However, it is difficult to overlap images on the correct plane because SPECT images are not sharp. In addition, because the marker definition was done manually, a small intra- and interobserver variability was possible. In the future, automated landmark selection will replace most of the manual landmark selection used in this study and should decrease the time required for fusion. Overall, the present study had some limitations. First, no lesions could be validated by histologic examination. All were validated by radiologic and clinical follow-up. This limitation was due to a selection bias toward patients presenting with occult metastasis not shown on conventional imaging or advanced disease without the need for lesion biopsy or surgery. Second, choosing the CT-scanning area on the basis of ^{131}I planar images and not on SPECT images might have led to missed lesions. Third, only 3 external markers were used. Further studies on the clinical usefulness of fusion images are needed, using more than 3 external markers and with precise coordination between anatomic and functional images.

CONCLUSION

For registration of anatomic and functional images in fusion imaging, the external-marker method of the present study was simple and practical. ^{131}I SPECT/CT fusion images obtained with this technique may improve the anatomically limited interpretation of ^{131}I scintigraphy alone for patients with differentiated thyroid carcinoma.

REFERENCES

1. Israel O, Keidar Z, Iosilevsky G, Bettman L, Sachs J, Frenkel A. The fusion of anatomic and physiologic imaging in the management of patients with cancer. *Semin Nucl Med.* 2001;31:191–205.
2. Townsend DW, Cherry SR. Combining anatomy and function: the path to true image fusion. *Eur Radiol.* 2001;11:1968–1974.
3. Hilton G, Pochin EE, Cunningham RM, et al. The role of radioiodine in the treatment of carcinoma of the thyroid. *Br J Radiol.* 1956;29:297–310.
4. Tyson JW, Wilkinson RH Jr, Witherspoon LR, et al. False positive ^{131}I total body scans. *J Nucl Med.* 1974;15:1052–1053.
5. Lang TF, Hasegawa BH, Liew SC, et al. Description of a prototype emission-transmission computed tomography imaging system. *J Nucl Med.* 1992;33:1881–1887.
6. Hasegawa BH, Wong KH, Iwata K, et al. Dual-modality imaging of cancer with SPECT/CT. *Technol Cancer Res Treat.* 2002;1:449–458.
7. Beyer T, Townsend DW, Brun T, et al. A combined PET/CT scanner for clinical oncology. *J Nucl Med.* 2000;41:1369–1379.
8. Fujita A, Hyodoh H, Kawamura Y, Kanegae K, Furuse M, Kanazawa K. Use of fusion images of I-131 metaiodobenzylguanidine, SPECT, and magnetic resonance studies to identify a malignant pheochromocytoma. *Clin Nucl Med.* 2000; 25:440–442.
9. Vansteenkiste JF, Stroobants SG, Dupont PJ, et al. FDG-PET scan in potentially operable non-small cell lung cancer: do anatometabolic PET-CT fusion images improve the localization of regional lymph node metastases? *Eur J Nucl Med.* 1998;25:1495–1501.

10. Kretschmer L, Altenvoerde G, Meller J, et al. Dynamic lymphoscintigraphy and image fusion of SPECT and pelvic CT-scans allow mapping of aberrant pelvic sentinel lymph nodes in malignant melanoma. *Eur J Cancer.* 2003;39:175–183.
11. Somer EJ, Marsden PK, Benatar NA, Goodey J, O'Doherty MJ, Smith MA. PET-MR image fusion in soft tissue sarcoma: accuracy, reliability and practicality of interactive point-based and automated mutual information techniques. *Eur J Nucl Med.* 2003;30:54–62.
12. Kessler ML, Pitluck S, Petti P, et al. Integration of multimodality imaging data for radiotherapy treatment planning. *Int J Radiat Oncol Biol Phys.* 1991;21:1653–1667.
13. Scott AM, Macapinlac H, Zhang J, et al. Image registration of SPECT and CT images using an external fiduciary band and three-dimensional surface fitting in metastatic thyroid cancer. *J Nucl Med.* 1995;36:100–103.
14. Perault C, Schvartz C, Wampach H, et al. Thoracic and abdominal SPECT-CT image fusion without external markers in endocrine carcinomas. *J Nucl Med.* 1997;38:1234–1242.
15. Even-Sapir E, Keidar Z, Sachs J, et al. The new technology of combined transmission and emission tomography in evaluation of endocrine neoplasms. *J Nucl Med.* 2001;42:998–1004.
16. Pietrzyk U, Herholz K, Fink G, et al. An interactive technique for three-dimensional image registration: validation for PET, SPECT, MRI and CT brain studies. *J Nucl Med.* 1994;35:2011–2018.